The Journal of Immunology

Cutting Edge: Signals from the B Lymphocyte Antigen Receptor Regulate MHC Class II Containing Late Endosomes

Karyn Siemasko, Bartholomew J. Eisfelder, Edward Williamson, Shara Kabak and Marcus R. Clark

J Immunol 1998; 160:5203-5208; ;
http://www.jimmunol.org/content/160/11/5203

The Journal of Immunology is published twice each month by
The American Association of Immunologists, Inc.,
1451 Rockville Pike, Suite 650, Rockville, MD 20852

Print ISSN: 0022-1767 Online ISSN: 1550-6606.

CUTTING EDGE

Cutting Edge: Signals from the B Lymphocyte Antigen Receptor Regulate MHC Class II Containing Late Endosomes[1]

Karyn Siemasko,* Bartholomew J. Eisfelder,* Edward Williamson,† Shara Kabak,* and Marcus R. Clark[2]*†

The B lymphocyte response to protein Ag is dependent upon the successful presentation to T cells of Ag-derived, MHC class II-restricted peptides. The B cell Ag receptor (BCR) facilitates this process by internalizing ligand and delivering it to specialized compartment(s) (MHC class II peptide-loading compartments (MIIC)) where it is processed into peptides and loaded onto MHC class II. In addition to efficiently targeting Ag, the BCR can provide tyrosine kinase-dependent signals that augment the presentation of Ag, possibly by enhancing the generation of immunogenic peptides. However, the mechanism by which this occurs is unclear. Herein, we report that the BCR signals a reorganization, fusion, and acidification of an MIIC-like compartment into an invariant chain- and MHC class II-rich complex of large vesicles. This complex becomes the primary target for endocytosed receptors. These data suggest that signals generated by the BCR regulate the site of Ag processing. ***The Journal of Immunology*****, 1998, 160: 5203–5208.**

The B cell Ag receptor (BCR)[3] is a multimeric receptor complex of membrane-bound Ig noncovalently associated with heterodimers of Ig-α and Ig-β. The cytoplasmic domains of these latter structures translate Ag engagement into cytoplasmic signaling events (1, 2). The receptor is activated by aggregation, which induces the juxtaposition of receptor-associated kinases, thereby initiating their transphosphorylation and activation. Among the immediate substrates phosphorylated are the conserved tyrosines found in the immunoreceptor tyrosine-based activation motif (ITAM) imbedded in the cytoplasmic tails of both Ig-α and Ig-β (3). These phosphotyrosines become the recruitment and activation sites for Fyn (4), Syk (5, 6), and possibly other tyrosine kinases. The proximal activation of kinases initiates divergent and interconnecting signaling cascades, of which the constituents include Erk, phospholipase C, Ras, and phosphatidylinositol 3 (PI 3)-kinase (7). In the periphery, the activation of these cascades can drive B cell proliferation, up-regulate surface activation markers, and increase Ab synthesis (8).

However, for Ig isotype switching, affinity maturation, and the generation of B cell memory, the signals generated by the BCR are not sufficient. T cell-derived lymphokines and surface ligands are also required (9). These costimulatory factors are provided by T cells capable of responding to MHC class II-restricted peptides displayed on the surface of Ag-stimulated B cells (10). The BCR facilitates formation of these MHC class II/peptide surface complexes by endocytosing and delivering Ag to compartments within the cell, where it is processed and loaded onto MHC class II (11–13). Although controversial, most studies have identified the site of peptide processing as specialized vesicles derived from late endosomes/early lysosomes (MIIC) which bear the marker designated lysosome-associated membrane protein (lamp-1) (14, 15). However, some Ags may be processed in vesicles that lie earlier in the endocytic pathway (16, 17).

Signals delivered by the BCR may also enhance the recruitment of T cell help. Polyvalent Ags are presented up to 50 times more efficiently than monovalent Ags, and this enhancement is not due to differences in internalization, subcellular targeting, or the up-regulation of costimulatory activity (18–20). Rather, it may be due to an increase in the degradation of endocytosed Ags (20). Although the mechanism by which this occurs is unclear, the observation that BCR ligation induces tyrosine phosphoproteins and GTP-binding proteins to associate with the MIIC (21) indicates that the site of Ag processing might be directly regulated by BCR initiated signaling cascades.

Herein, we report that signals emanating from the BCR induce the redistribution, fusion, and acidification of lamp-1$^+$ endosomal vesicles to form an acidic perinuclear complex containing a majority of the detectable MHC class II within the cytoplasm. These data indicate that the signaling capacities of the BCR may enhance

Section of Rheumatology and Departments of *Medicine and †Pathology, Committee on Immunology, University of Chicago, Chicago, IL 60637

Received for publication March 4, 1998. Accepted for publication March 25, 1998.

The costs of publication of this article were defrayed in part by the payment of page charges. This article must therefore be hereby marked *advertisement* in accordance with 18 U.S.C. Section 1734 solely to indicate this fact.

[1] M.R.C. is supported by grants from the National Institutes of Health (GM52736, GM56187) and the Arthritis Foundation. S.K. is supported by a grant from the Lucille P. Markey Charitable Trust. K.S. is supported by a Cardiovascular Sciences Training Grant (5T32HL0738117).

[2] Address correspondence and reprint requests to Dr. Marcus Clark, University of Chicago, Department of Medicine, MC0930, Chicago, IL 60637. E-mail address: mclark@medicine.bsd.uchicago.edu

[3] Abbreviations used in this paper: BCR, B cell Ag receptor; PI 3, phosphatidylinositol 3; IMDM, Iscove's modified Dulbecco's medium; TfR, transferrin receptor; lamp-1, lysosome-associated membrane protein; PE, phycoerythrin; Ii, invariant chain; PKC, protein kinase C; MCII, MHC class II peptide-loading compartment.

0022-1767/98/$02.00

the presentation of Ag by regulating the subcellular compartment in which processing and MHC class II loading occurs.

Materials and Methods

Cell lines and Abs

The A20/IIA1.6 B cell line was maintained in Iscove's modified Dulbecco's medium (IMDM) (Life Technologies, Grand Island, NY) supplemented with 10% FCS (HyClone, Logan, UT), 2 mM glutamine, 100 U/ml penicillin, and 100 μg/ml streptomycin at 37°C in 7.5% CO_2.

Rabbit antisera (ABCYTB) was raised against a peptide (CQKGPRGPPPAGLLQ) from the cytoplasmic tail of the mouse MHC class II β-chain. ID4B and In-1 were provided by Andrea Sant (University of Chicago). The following Abs were purchased: FITC-conjugated anti-goat IgG, FITC-conjugated goat anti-rat IgG, phycoerythrin (PE)-conjugated donkey anti-rat IgG, FITC-conjugated donkey anti-rabbit IgG, rabbit anti-mouse IgG, and rat anti-goat IgG (all from Jackson ImmunoResearch, West Grove, PA); goat anti-mouse IgG2a and biotinylated goat anti-mouse IgG2a (Southern Biotechnology Birmingham, AL); FITC-conjugated anti-rat IgG2b and biotinylated anti-rat IgG2a (Binding Site, Birmingham, U.K.); 15-nm gold-conjugated goat anti-rat IgG and 5-nm gold-conjugated rabbit anti-goat IgG (British Biocell International, Cardiff, U.K.); goat anti-rat IgG (H+L) (ICN, Costa Mesa, CA); and rabbit anti-horse ferritin (Sigma, St. Louis, MO).

Confocal microscopy

For BCR/lamp-1 costaining, A20/IIA1.6 cells were first incubated with 10 μg/ml goat anti-mouse IgG2a (αBCR) Abs at 4°C for 10 min, washed, then incubated with anti-goat IgG-FITC (1:100) and washed again. Cells were then warmed to 37°C for 0, 15, or 30 min, fixed with 3% paraformaldehyde/3% sucrose, and permeabilized with 0.05% saponin essentially as described (22). Samples were then incubated with ID4B for 1 h at room temperature, washed, and then incubated with anti-rat IgG-PE (1:100). To label cells with ferritin, they were washed in ice-cold serum-free IMDM, resuspended with 0.25 mg/ml cationized ferritin (Sigma) in IMDM, and incubated on ice for 10 min. Cells were then warmed to 37°C for 30 min, washed, and then resuspended on ice. Following sequential incubation with goat anti-mouse IgG2a and donkey anti-goat IgG-FITC, cells were warmed to 37°C for 30 min, then washed, fixed, and stained with anti-ferritin Abs followed by anti-rabbit-FITC Abs. Acidic compartments were visualized by incubating samples with 500 nM Lysosensor dye (Molecular Probes, Eugene, OR) at 37°C for 1 h. To stain for invariant chain (Ii), samples were pretreated with 400 μg/ml leupeptin for 2 h before stimulation. Confocal sections of approximately 0.75 to 1.0 μm were acquired using a Zeiss 410 confocal microscope and displayed by pseudocoloring using LSM software (Zeiss, Oberkochen, Germany). All experiments were performed at least three times by two investigators working independently (K.S. and B.J.E.).

To test for inhibition of lamp-1^+ vesicle aggregation formation, cells were treated with genistein (Life Technologies) for 15 min at 100 μg/ml, wortmannin (Sigma) for 10 min at 1 μM, or staurosporin for 12 h at 1 μM (Calbiochem, San Diego, CA) before BCR cross-linking with 10 μg/ml anti-mouse IgG2a. Induction of vesicle activation without receptor engagement was tested by stimulating cells with 10 ng/ml PMA, 1 μM ionomycin, or both together for 15 min at 37°C. Induction of aggregation was quantitated by scoring 10 random confocally scanned fields (~100 cells).

Electron microscopy

Cells were stimulated for 15 min with anti-IgG, as described above, or with rabbit anti-IgG (10 μg/ml), followed by 5-nm gold particle-conjugated donkey anti-rabbit IgG (1:4 dilution), then fixed in 8% formaldehyde/250 mM HEPES, pH 7.2. Cells were infiltrated with 2.3 M sucrose, frozen in liquid nitrogen, and sectioned at −110°C. For immunostaining, samples were blocked in 10% FCS/0.12% glycine/PBS at room temperature for 30 min, then incubated with ID4B at a 1:2 dilution for 30 min, and then washed two times in PBS/0.12% glycine. Samples were then incubated with 15-nm gold particle-conjugated-goat anti-rat IgG. After washing with PBS/glycine and distilled water, the grids were incubated with a 1.8% methyl cellulose/0.3% uranyl acetate solution. Samples were visualized using a JEOL 100 CX transmission electron microscope (JOEL, Peabody, MA) at an accelerating voltage of 60 kV (23).

Estimation of the distribution vesicle size

Random sequential images from ID4B-stained electron microscopic samples, which contained lamp-1^+ structures with discernible membranes, were printed at a final magnification of ×21,000. The long (l) and short (s) diameter of each lamp-1^+ vesicle was measured in mm, and the relative volume of each was estimated by the equation $[(l + s)/2]^3\pi$. Fifty vesicles were quantitated in the unstimulated group and 100 in the stimulated group.

Stereology

From two grids for each sample, a typical field of cells was selected. A sequential and contiguous series of photomicrographs (×34,000, final magnification) was obtained (~75 per series, 300 total), which encompassed the field within the relevant grid space. Given that the orientation of cells sampled was random and therefore isotropic, volume estimations of the lamp-1^+-staining vesicles and of the total cell were determined by point counting. To determine the surface area of the lamp-1^+ vesicles, test line intersections crossing the positive-staining vesicle membrane were counted, and the ratio of the lamp-1^+ vesicle surface area to the total cell volume was determined (23).

Results and Discussion

The BCR induces the aggregation and fusion of late endosomes/lysosomes. In addition to being an "engine" that drives pathways of signal transduction (24), the BCR mediates efficient class II-restricted presentation to T cells of peptides derived from receptor-bound Ag (12, 13). Although the activation and presentation capabilities of the BCR are often considered separately, we postulated that they might be interrelated and that signals initiated by the BCR might facilitate the ability of cells to process and present Ag. To address this possibility directly, we used confocal and electron microscopy to examine whether the compartments or molecules involved in Ag presentation change in character or distribution in response to BCR perturbation. We began our investigations by examining lamp-1^+ endocytic vesicles because they have been implicated previously as the site of Ag processing and peptide loading (11, 14).

The murine B cell line A20 IIA1.6, which lacks FcγRII (25), was stimulated with FITC-conjugated polyclonal anti-IgG Abs for various times at 37°C, then fixed, permeabilized, and stained with Abs to the late endosome/lysosome marker, lamp-1 (ID4B) (14, 26). As shown in Figure 1*A* (*upper panels*), unstimulated cells had several small lamp-1-bearing vesicles (red) distributed throughout the cytoplasm. Following ligation of the BCR, there was a remarkable redistribution of these vesicles such that by 15 min they formed a single large perinuclear aggregate in 40 to 50% of the cells, which contained 80% or more of the lamp-1^+ vesicles. These aggregates became the primary target for the endocytosed ligated BCR complexes (colocalization shown in yellow). The coalescence of lamp-1^+ vesicles began as early as 5 min and preceded the arrival of detectable amounts of endocytosed BCR complexes (data not shown) indicating that coalescence was not occurring in response to the delivery of endocytosed complexes. Furthermore, the aggregation of vesicles persisted for at least 4 h, during which time the aggregate contained the majority of detectable BCR complexes in the cell (data not shown).

We then asked whether the coalescence of lamp-1-bearing vesicles was a specific consequence of BCR ligation. We first examined the transferrin receptor (TfR), which, although it recycles through early endosomes when bound to ligand, is driven to late endosomes/lysosomes when cross-linked with anti-receptor Abs (27). As seen in Figure 1*A* (*middle panels*), although the TfR complex was internalized efficiently and colocalized with some of the lamp-1 vesicles (arrow), it did not induce their coalescence. These data indicate that the simple delivery of an aggregated receptor to the lamp-1-bearing compartment is not sufficient to induce its coalescence.

Since the expression of lamp-1 is restricted to late endosomes and lysosomes, we next asked whether other compartments were responsive to BCR ligation. Therefore, we first labeled the entire endocytic pathway in A20IIA1.6 cells with cationized ferritin and then stained unstimulated and stimulated populations with anti-

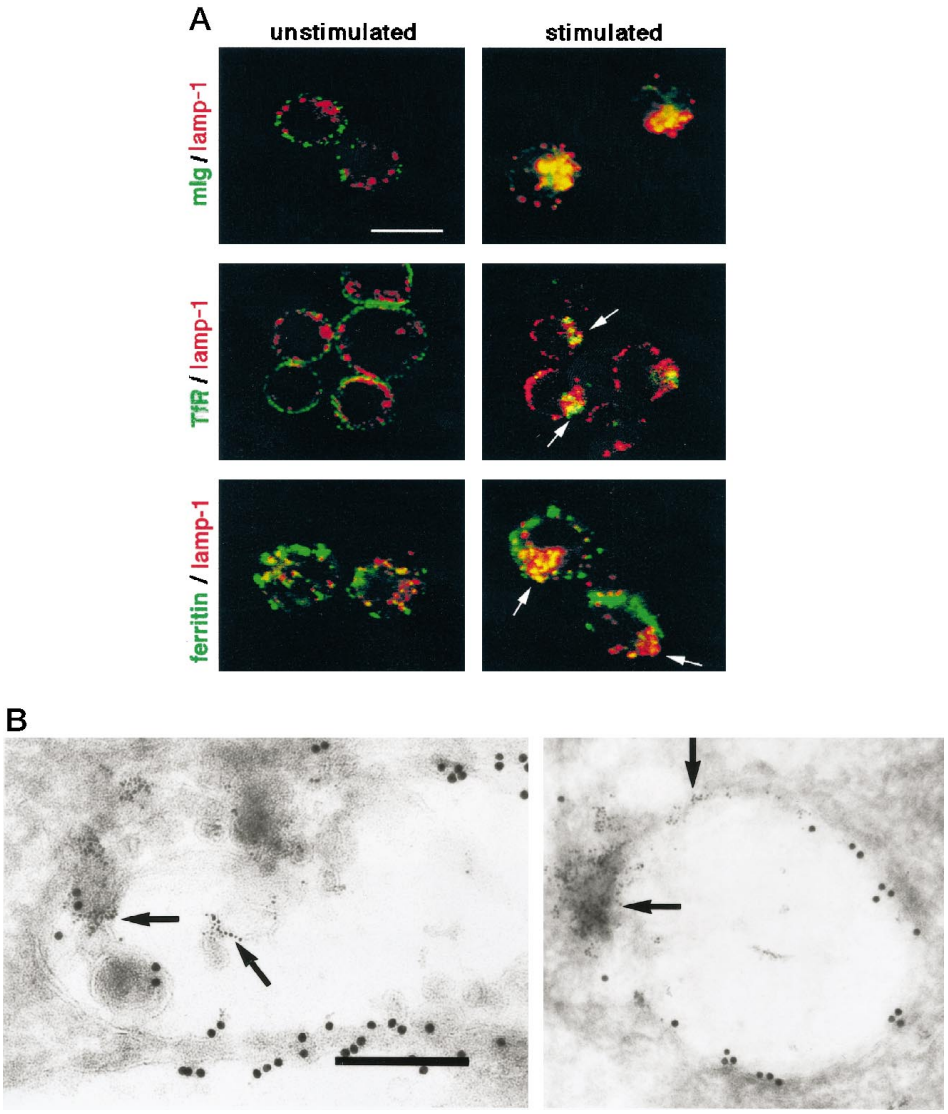

FIGURE 1. The BCR specifically induces the translocation of late endosomes/lysosomes to form a complex that colocalizes with internalized receptor complexes. *A*, *upper panels*, Confocal micrographs demonstrating that lamp-1$^+$ vesicles (ID4B, red) of A20IIA1.6 cells aggregate following BCR (green) perturbation with anti-IgG Abs and by 15 min colocalize with internalized receptor complexes (yellow); *middle panels*, cross-linked and internalized TfR complexes (green) colocalize with lamp-1$^+$ vesicles (red) but do not induce their redistribution; *lower panels*, BCR stimulation induces the translocation of only a subset of the endocytic pathway. Cells were continuously loaded for 30 min with cationized ferritin and then stimulated with Abs to the BCR. Following stimulation and washing, cells were fixed and stained with Abs to ferritin (green) and ID4B (red). Scale bar, 10 μm. *B*, Immunoelectron micrographs of stimulated cells demonstrating internalized BCR complexes (5-nm gold particles, arrows) within lamp-1$^+$ vesicles (15-nm gold particles). Micrograph on *left* shows internalized BCR complexes within a multimembranous intraluminal body of a lamp-1$^+$ vesicle, while the image on the *right* demonstrates BCR complexes in a vesicle wall. Scale bar, 0.3 μm.

ferritin and anti-lamp-1 Abs. As seen in Figure 1*A* (*bottom panels*), the lamp-1$^+$ vesicles constituted only ~25 to 50% of the endosomes in resting cells. Upon stimulation, only the lamp-1$^+$/ferritin$^+$ subpopulation of vesicles aggregated, indicating that early endosomes are not responsive to BCR perturbation. Similar results were obtained when samples were stained for the early endosomal marker, TfR (data not shown). These data demonstrate that the BCR responsive compartment is restricted to late endosomes/lysosomes and that these vesicles are part of the normal endocytic pathway.

The extinguishing of anti-Ig-FITC and anti-lamp-1-PE to yellow in BCR-stimulated cells indicated that most of the endocytosed BCR complexes were contained within the lamp-1$^+$-aggregated vesicles. However, to exclude the possibility that coregionalization and not colocalization was occurring, we performed immunoelectron microscopy. The BCR on A20 cells was labeled by first incubating cells on ice with rabbit anti-mouse IgG2a, followed by 5-nm gold particle-conjugated anti-rabbit IgG. The cells were then stimulated by warming to 37°C for 20 min and fixed, and then frozen sections were prepared and stained with ID4B (15-nm gold). In stimulated cells, large lamp-1$^+$ vesicles were found, many in excess of 1 μm in diameter (Fig. 1*B*). Many of these vesicles contained multimembranous intraluminal bodies, reminiscent of those described in late endosomes (28). Most of the internalized BCR complexes detected within the lamp-1$^+$ vesicles were within the intraluminal bodies (*left panel*). Less frequently, internalized IgG complexes were found within the vesicle wall (*right panel*). Surprisingly, large lamp-1$^+$ vesicles were absent in unstimulated cells, suggesting that the BCR was inducing fusion within the lamp-1$^+$ compartment. To explore this possibility, we used immunoelectron microscopy to examine the size distribution of lamp-1$^+$ vesicles in unstimulated and BCR stimulated cells.

BCR signals vesicular coalescence

We began our analysis by measuring all of the lamp-1$^+$ membrane-bound structures found in random fields of electron micrographic images from unstimulated and stimulated cells. The relative volume of each structure was then estimated from their average radius. As shown in Figure 2*A*, only small vesicles with average volumes of 190 (arbitrary units) were observed in unstimulated cells (total vesicles counted, $n = 50$). These vesicles had an average radius of ~40 nm and they lacked the intraluminal bodies seen within the vesicles of stimulated cells (data not shown). When we examined stimulated cells, two new populations of larger vesicles were observed ($n = 100$). One intermediate population, which constituted 15% of the total vesicles, had an average

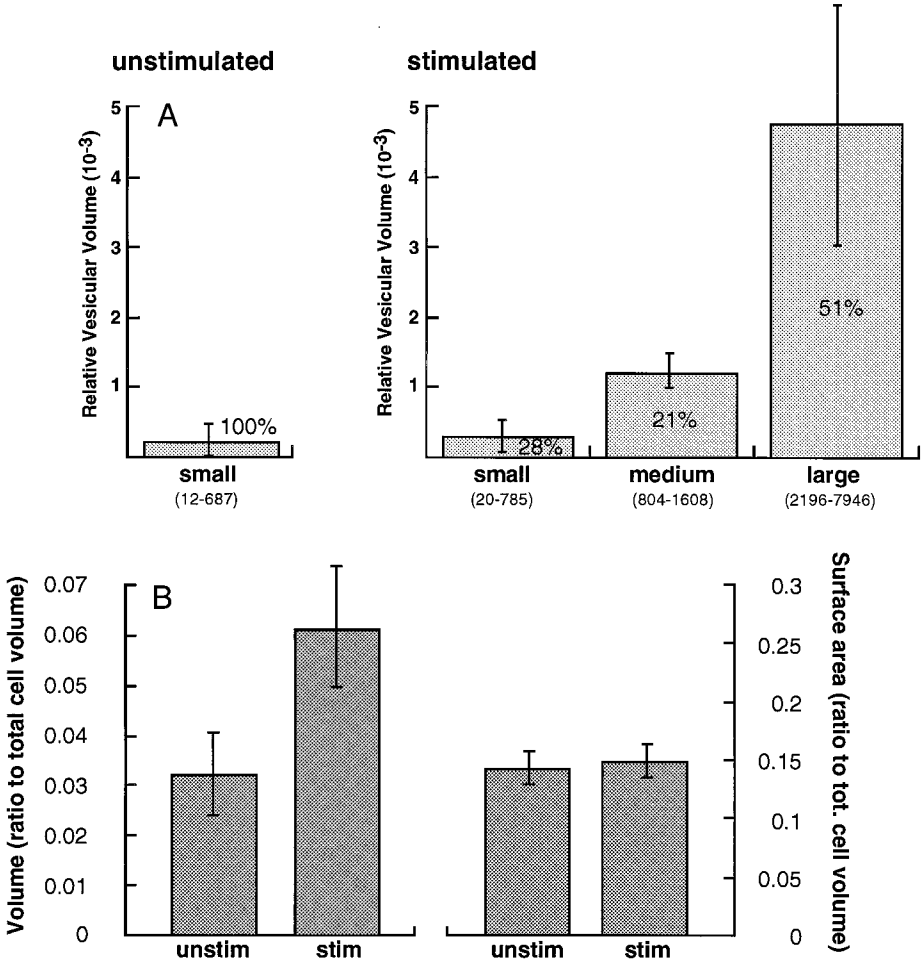

FIGURE 2. Stimulation of the BCR induces the fusion of lamp-1-bearing endocytic vesicles. *A*, The size distribution of lamp-1$^+$ vesicles changes with BCR perturbation. Following stimulation, >70% of lamp-1$^+$ vesicular volume is contained within new medium or large-size vesicles. The size of vesicles in each sample population was estimated from random electron photomicrographs. Shown are the relative mean volume and SDs for each population, the percentage of total volume each category of vesicle contains, and range of volumes for each category (the latter is shown in parentheses). *B*, The volume of the lamp-1$^+$ compartment increases, while the surface area remains the same. The volume and surface area of the lamp-1$^+$ compartment were estimated from sequential and contiguous electron photomicrographs of samples from unstimulated and stimulated cells stained with Abs to lamp-1. Shown are the relative values for the volume and surface area corrected for total assayed cell volume. Error bars represent SE of the mean.

volume of 1120. The second population, which constituted 9% of the total, consisted of very large vesicles with an average relative volume of 4750. Although only a minority of the vesicles in stimulated cells were either intermediate or large in size, they contained >70% of the luminal volume of the lamp-1$^+$ population.

The rapidity with which these large lamp-1$^+$ vesicles formed indicates that they did not arise from de novo biosynthesis. However, these data do not indicate whether the large vesicles arose primarily from homotypic fusion of lamp-1$^+$ vesicles, from heterotypic fusion, or merely from swelling of preexisting vesicles. In all three cases, it would be expected that the total volume of the lamp-1$^+$ compartment would increase. However, with heterotypic fusion or swelling, the total surface area of the lamp-1$^+$ compartment would increase, while if homotypic fusion was occurring, it would remain the same. Therefore, to determine whether fusion of the lamp-1$^+$ vesicles occurred following BCR stimulation, quantitative stereology was used to assay the volume and surface area of the lamp-1$^+$ compartments in unstimulated and stimulated cells (23). After stimulation and fixation, isotropic sections were cut and stained with ID4B, followed by 15-nm gold particle-conjugated anti-rat IgG; stereology was done on micrographs of randomly sampled sections. The volume of the entire lamp-1$^+$ compartment was estimated by summing the point-sampled intercepts lying within labeled vesicles, while surface area was determined from the relative number of test lines that intersected with their membranes. These values were then corrected for the total cell volume in each sampled population. As shown in Figure 2*B*, following stimulation the volume of the lamp-1$^+$ compartment increased by ~1.9-fold, while the surface area between the two groups did not change. It might have been predicted that the fusion of transport structures bearing endocytosed BCR complexes with the lamp-1$^+$ compartment would increase its' overall surface area. However, most of the endocytosed complexes were found in intraluminal bodies (Fig. 1*B*) and therefore did not contribute to the limiting wall of the vesicles.

We next asked whether the coalescence of lamp-1$^+$ vesicles occurred in response to biochemical signals generated by the BCR. Since all known signaling functions of the BCR are dependent on tyrosine kinase activation (29), we first determined whether the tyrosine kinase inhibitor genistein would affect coalescence. As seen in Figure 3, preincubation of cells with genistein inhibited the ability of the BCR to induce the coalescence of lamp-1$^+$ vesicles. We next assayed for which tyrosine kinase-dependent pathway(s) might be involved. PI 3-kinase seemed to be a good candidate because it has been implicated in a myriad of cellular processes including the fusion of early endosomes (30). However, pretreatment of cells with the PI 3-kinase inhibitor wortmannin had no effect on lamp-1$^+$ vesicular coalescence. In contrast, treatment with PMA and ionomycin, which can recapitulate the signaling activities of the Ag receptors (31), strongly induced coalescence. PMA alone induced a partial response, while ionomycin alone did not (data not shown). These observations suggest that PKC, which is downstream of both Ras and phospholipase Cγ, may be involved (32). Indeed, preincubation with the PKC inhibitor staurosporin inhibited coalescence. These data indicate that the activation of

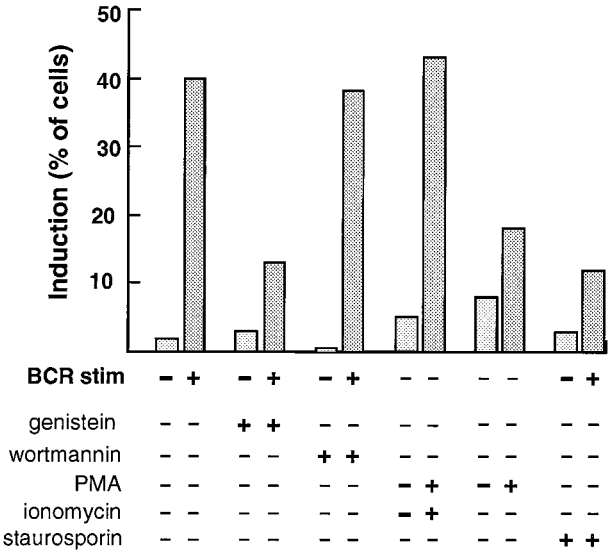

FIGURE 3. BCR-induced coalescence of lamp-1$^+$ vesicles is blocked by inhibitors of signal transduction. The BCR on A20/IIA1.6 cells was cross-linked in the presence of the indicated inhibitors or treated with PMA ± ionomycin for 15 min, then fixed and stained with ID4B. Cells in which >80% of the lamp-1$^+$ vesicles were aggregated were scored as positive. Ten random fields (100 cells total) were scored. Most cells (>90%) treated with either anti-IgG or PMA/ionomycin had some degree of lamp-1$^+$ vesicle aggregation.

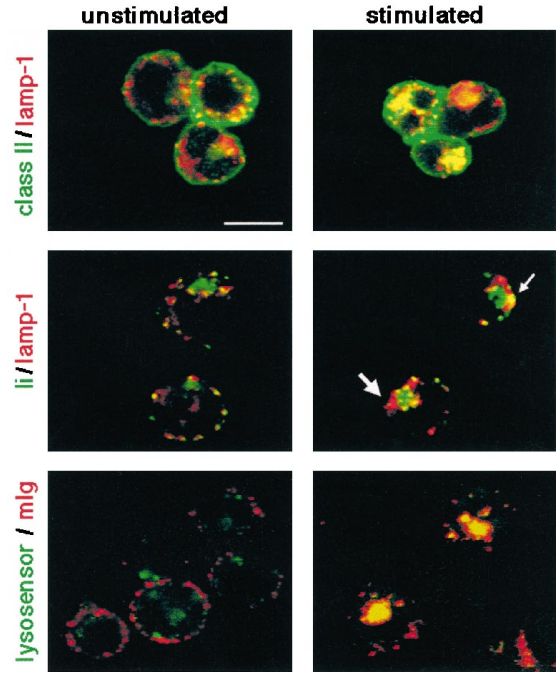

FIGURE 4. The aggregate of lamp-1$^+$ vesicles is an acidic compartment rich in MHC class II and Ii. Unstimulated cells and cells stimulated for 15 min with anti-IgG were fixed and stained with either Abs to the cytoplasmic tail of MHC class IIβ and ID4B (*upper panels*) or In-1(Ii) and ID4B (*middle panels*). In the *lower panels*, cells were labeled with Lysosensor, which fluoresces green in acidic environments (pKa = 5.2) and Abs against surface anti-IgG (red).

PKC by one or more pathways may be necessary for vesicular coalescence.

Fusion occurs within a subcellular compartment that has the characteristics required for peptide processing and MHC class II loading

Our observation that the BCR traffics to and persists within the coalescence of lamp-1$^+$ vesicles suggests a role for the vesicular complex in Ag presentation. Therefore, unstimulated and stimulated cells were stained with Abs to the cytoplasmic tail of the β-chain of MHC class II (green) and lamp-1 (red). In unstimulated cells, there was bright staining for MHC class II molecules on the plasma membrane, while most of the cytoplasmic MHC class II was found within a subset of the lamp-1$^+$ vesicles (Fig. 4, *top panels*). Upon receptor stimulation, the cytoplasmic MHC class II redistributed to the same lamp-1$^+$ complex (Fig. 4) targeted by the BCR (data not shown). This compartment also contains Ii, which is necessary for the stabilization of newly synthesized MHC class II and its transport to the peptide loading compartment (Fig. 4, *bottom panels*). Interestingly, within the complex there are distinctly Ii$^+$ (small arrow) and Ii$^-$ (large arrow) subcompartments. Thus, this complex of vesicles contains Ag, MHC class II, and Ii, giving it the essential characteristics that have defined other peptide loading compartments. The compartment is derived from late endosomes and therefore most closely resembles the previously described MIIC compartment (14, 33).

The above data demonstrate that the BCR induces the formation of, and is targeted to, a subcellular complex rich in MHC class II and Ii molecules. We investigated whether an acidic environment, which is necessary for Ii release, protein degradation, and class II loading (12, 34), was present. BCR-stimulated and -unstimulated cells were costained with PE-conjugated anti-IgG and Lysosensor, a vital dye that fluoresces green at acidic pH levels (pKa = 5.2). In resting cells, there was diffuse, dim staining of the cytoplasm with a few small acidic vesicles located peripherally (Fig. 4, *bottom panels*). Upon stimulation, large new acidic structures formed, which colocalized with internalized receptor (yellow). Costaining with ID4B and another acidic dye that can stain permeabilized cells (Lysosensor, Molecular Probes) demonstrated that the newly acidified structure costained with lamp-1 (data not shown).

In summary, the BCR is capable of generating tyrosine kinase-dependent signals that regulate both the physical and biochemical properties of an MIIC-like compartment. It is easy to understand how decreasing the pH of the processing compartment could facilitate Ag degradation. The benefits associated with the aggregation and fusion of constituent compartment vesicles is less evident. However, fusion within the lamp-1$^+$ aggregate does not simply result in larger homogenous vesicles. Rather, as demonstrated by the heterogeneous distribution of Ii, it establishes different complex microenvironments in proximity to one another. This may allow the different processes involved in the generation of MHC class II/peptide complexes, such as Ii degradation and peptide loading, to occur under conditions that are optimal for each (35).

Acknowledgments

We thank Drs. Jan Burkhardt, Andrea Sant, Yair Argon, and Jim Miller for their helpful comments on this manuscript.

References

1. Tseng, J., Y. J. Lee, B. J. Eisfelder, and M. R. Clark. 1994. The B cell antigen receptor complex: mechanisms and implications of tyrosine kinase activation. *Immunol. Res. 13:299.*
2. Reth, M., and J. Wienands. 1997. Initiation and processing of signals from the B cell antigen receptor. *Annu. Rev. Immunol. 15:453.*
3. Cambier, J. C. 1995. New nomenclature for the Reth motif (or ARH1/TAM/ARAM/YXXL). *Immunol. Today 16:110.*
4. Clark, M. R., S. A. Johnson, and J. C. Cambier. 1994. Analysis of Ig-alpha tyrosine kinase interaction reveals two levels of binding specificity and tyrosine phosphorylated Ig-alpha stimulation of Fyn activity. *EMBO J. 13:1911.*

5. Rowley, R. B., A. L. Burkhardt, H. G. Chao, G. R. Matsueda, and J. B. Bolen. 1995. Syk protein-tyrosine kinase is regulated by tyrosine-phosphorylated Ig alpha/Ig beta immunoreceptor tyrosine activation motif binding and autophosphorylation. *J. Biol. Chem. 270:11590.*
6. Kurosaki, T., S. A. Johnson, L. Pao, K. Sada, H. Yamamura, and J. C. Cambier. 1995. Role of the Syk autophosphorylation site and SH2 domains in B cell antigen receptor signaling. *J. Exp. Med. 182:1815.*
7. DeFranco, A. L. 1997. The complexity of signaling pathways activated by the BCR. *Curr. Opin. Immunol. 9:296.*
8. Cambier, J. C., and J. T. Ransom. 1987. Molecular mechanisms of transmembrane signaling in B lymphocytes. *Annu. Rev. Immunol. 5:175.*
9. Liu, Y. J., and J. Banchereau. 1997. Regulation of B-cell commitment to plasma cells or to memory B cells. *Semin. Immunol. 9:235.*
10. Clark, E. A., and J. A. Ledbetter. 1994. How B-cells and T-cells talk to each other. *Nature 367:425.*
11. Watts, C. 1997. Capture and processing of exogenous antigens for presentation on MHC molecules. *Annu. Rev. Immunol. 15:821.*
12. Cresswell, P. 1994. Assembly, transport, and function of MHC class II molecules. *Annu. Rev. Immunol. 12:259.*
13. Germain, R. N. 1994. MHC-dependent antigen processing and peptide presentation: providing ligands for T-lymphocyte activation. *Cell 76:287.*
14. Peters, P. J., J. J. Neefjes, V. Oorschot, H. L. Ploegh, and H. J. Geuze. 1991. Segregation of MHC II molecules from MHC I molecules in the Golgi complex for transport to lysosomal compartments. *Nature 349:669.*
15. Rudensky, A. V., M. Maric, S. Eastman, L. Shoemaker, P. C. DeRoos, and J. S. Blum. 1994. Intracellular assembly and transport of endogenous peptide-MHC class II complexes. *Immunity 1:585.*
16. Pierre, P., L. K. Denzin, C. Hammond, J. R. Drake, S. Amigorena, P. Cresswell, and I. Mellman. 1996. HLA-DM is localized to conventional and unconventional MHC class II-containing endocytic compartments. *Immunity 4:229.*
17. Castellino, F., and R. N. Germain. 1995. Extensive trafficking of MHC-class II-invariant chain complexes in the endocytic pathway and appearance of peptide-loaded class II in multiple compartments. *Immunity 2:73.*
18. Casten, L. A., and S. K. Pierce. 1988. Receptor-mediated B cell antigen processing: increased antigenicity of a globular protein covalently coupled to antibodies specific for B cell surface structures. *J. Immunol. 140:404.*
19. Tony, H.-P., and D. C. Parker. 1985. Major histocompatibility complex-restricted, polyclonal B cell responses resulting from helper T cell recognition of antiimmunoglobulin presented by small B lymphocytes. *J. Exp. Med. 161:223.*
20. Song, W., H. Cho, P. Cheng, and S. K. Pierce. 1995. Entry of B cell antigen receptor and antigen into class II peptide-loading compartment is independent of receptor cross-linking. *J. Immunol. 155:4255.*
21. Xu, X., B. Press, N. M. Wagle, H. Cho, A. Wandinger-Ness, and S. K. Pierce. 1996. B cell antigen receptor signaling links biochemical changes in the class II peptide-loading compartment to enhanced processing. *Int. Immunol. 8:1867.*
22. Kupfer, H., C. R. Monks, and A. Kupfer. 1994. Small splenic B cells that bind to antigen-specific T helper (Th) cells and face the site of cytokine production in the Th cells selectively proliferate: immunofluorescence microscopic studies of Th-B antigen presenting cell interactions. *J. Exp. Med. 179:1507.*
23. Griffiths, G. 1993. *Fine Structure Immunocytochemistry*. Springer-Verlag, Berlin.
24. Pleiman, C. M., D. D'Ambrosio, and J. C. Cambier. 1994:. The B-cell antigen receptor complex: structure and signal transduction. *Immunol. Today 15:393.*
25. Jones, B., J. P. Tite, and C. A. J. Janeway. 1986. Different phenotypic variants of the mouse B cell tumor A20/2J are selected by antigen- and mitogen-triggered cytotoxicity of L3T4-positive, I-A-restricted t cell clones. *J. Immunol. 136:348.*
26. Chen, J. W., T. L. Murphy, M. C. Willingham, I. Pastan, and J. T. August. 1985. Identification of two lysosomal membrane glycoproteins. *J. Cell Biol. 101:85.*
27. Weissman, A. M., R. D. Klausner, K. Rao, and J. B. Harford. 1986. Exposure of K562 cells to anti-receptor monoclonal antibody OKT9 results in rapid redistribution and enhanced degradation of the transferrin receptor. *J. Cell Biol. 102:951.*
28. Griffiths, G., R. Matteoni, R. Back, and B. Hoflack. 1990. Characterization of the cation-independent mannose 6-phosphate receptor-enriched prelysosomal compartment in NRK cells. *J. Cell Sci. 95:441.*
29. Gold, M. R., D. A. Law, and A. L. DeFranco. 1990. Stimulation of protein tyrosine phosphorylation by the B-lymphocyte antigen receptor. *Nature 345:810.*
30. Ward, S. G., C. H. June, and D. Olive. 1996. PI 3-kinase: a pivotal pathway in T-cell activation? *Immunol. Today 17:187.*
31. Cambier, J. C., and J. T. Ransom. 1987. Early events in B cell activation. *Annu. Rev. Immunol. 5:175.*
32. Cantrell, D. 1996. T cell antigen receptor signal transduction pathways. *Annu. Rev. Immunol. 14:259.*
33. West, M. A., J. M. Lucocq, and C. Watts. 1994. Antigen processing and class II MHC peptide-loading in human B-lymphoblastoid cells. *Nature 369:147.*
34. McCoy, K. L., J. Miller, M. Jenkins, F. Ronchese, R. N. Germain, and R. H. Schwartz. 1989. Diminished antigen processing by endosomal acidification mutant antigen-presenting cells. *J. Immunol. 143:29.*
35. Ferrari, G., A. M. Knight, C. Watts, and J. Pieters. 1997. Distinct intracellular compartments involved in invariant chain degradation and antigenic peptide loading of major histocompatibility complex (MHC) class II molecules. *J. Cell Biol. 139:1433.*